Stimulation of microtubule-based transport by nucleation of microtubules on pigment granules

Irina Semenova[a], Dipika Gupta[a], Takeo Usui[b], Ichiro Hayakawa[c], Ann Cowan[a], and Vladimir Rodionov[a,*]

[a]R. D. Berlin Center for Cell Analysis and Modeling and Department of Cell Biology, UConn Health, Farmington, CT 06030; [b]Faculty of Life and Environmental Sciences, University of Tsukuba, Ibaraki 305-8572, Japan; [c]Division of Applied Chemistry, Graduate School of Natural Science and Technology, Okayama University, Okayama 700-8530, Japan

ABSTRACT **Microtubule (MT)-based transport can be regulated through changes in organization of MT transport tracks, but the mechanisms that regulate these changes are poorly understood. In *Xenopus* melanophores, aggregation of pigment granules in the cell center involves their capture by the tips of MTs growing toward the cell periphery, and granule aggregation signals facilitate capture by increasing the number of growing MT tips. This increase could be explained by stimulation of MT nucleation either on the centrosome or on the aggregate of pigment granules that gradually forms in the cell center. We blocked movement of pigment granules to the cell center and compared the MT-nucleation activity of the centrosome in the same cells in two signaling states. We found that granule aggregation signals did not stimulate MT nucleation on the centrosome but did increase MT nucleation activity of pigment granules. Elevation of MT-nucleation activity correlated with the recruitment to pigment granules of a major component of MT-nucleation templates, γ-tubulin, and was suppressed by γ-tubulin inhibitors. We conclude that generation of new MT transport tracks by concentration of the leading pigment granules provides a positive feedback loop that enhances delivery of trailing granules to the cell center.**

Monitoring Editor
Xueliang Zhu
Chinese Academy of Sciences

Received: Aug 4, 2016
Revised: Mar 27, 2017
Accepted: Mar 29, 2017

INTRODUCTION

Microtubule (MT)-based transport is critical for endomembrane trafficking, neuronal signaling, and mitosis (Caviston and Holzbaur, 2006; Walczak *et al.*, 2010; Kapitein and Hoogenraad, 2011). Movement of organelles and particles along cytoplasmic MTs is powered by MT motors: plus end–directed kinesins and minus end–directed dynein (Vale, 2003). MT-based transport is generally regulated by fine-tuning the activities of opposing MT motors bound to the same cargo organelles (Verhey and Hammond, 2009; Akhmanova and Hammer, 2010; Barlan *et al.*, 2013; Fu and Holzbaur, 2014). However, regulation may also entail changes in the availability of MT tracks for transport. A remarkable example of this type of MT transport regulation is provided by *Xenopus* melanophores.

The main function of *Xenopus* melanophores is fast and synchronous redistribution of thousands of pigment granules that either accumulate in the cell center (pigment aggregation) or uniformly distribute throughout the cytoplasm (pigment dispersion). During pigment aggregation, pigment granules moving along randomly arranged actin filaments are captured by the growing tips of radial MTs for rapid delivery to the cell center by dynein motors (Lomakin *et al.*, 2009). We found previously that pigment aggregation signals enhanced granule capture by increasing the number of MT tips growing from the cell center (Lomakin *et al.*, 2011). However, how pigment aggregation signals increase the number of growing MT tips remained unknown.

Growth of MTs from the cell center is generally explained by MT nucleation on the centrosome. It is therefore possible that pigment aggregation signals increase the number of MTs growing to the cell periphery by stimulating centrosome MT nucleation activity. Pigment aggregation is triggered by a decrease in the cytoplasmic levels of cAMP and activity of protein kinase A (PKA; Kashina and Rodionov, 2005). Therefore stimulation of MT nucleation on the centrosome

This article was published online ahead of print in MBoC in Press (http://www.molbiolcell.org/cgi/doi/10.1091/mbc.E16-08-0571) on April 5, 2017.

*Address correspondence to: Vladimir Rodionov (rodionov@ uchc.edu).

Abbreviations used: CLASP, cytoplasmic linker associated protein; MSH, melanocyte-stimulating hormone; MT, microtubule; γ-TuRC, γ-tubulin ring complex.

Supplemental Material can be found at:
http://www.molbiolcell.org/content/suppl/2017/04/03/mbc.E16-08-0571v1.DC1

could be caused by a drop in PKA activity. Supporting a role in regulation of MT nucleation, PKA is scaffolded to the centrosome by AKAPs AKAP450/AKAP350/CG-NAP and kendrin (Witczak *et al.*, 1999; Flory *et al.*, 2000; Takahashi *et al.*, 2000; Li *et al.*, 2001; Terrin *et al.*, 2012). However, regulation of MT nucleation on the centrosome by PKA has never been demonstrated directly.

An increase in the number of MTs growing to the cell periphery could be also explained by the nucleation of MTs on pigment granules accumulating in the cell center. Our previous studies showed that cytoplasmic fragments of fish melanophores lacking the centrosome formed a polarized radial array with the pigment granule aggregate in the center (Rodionov and Borisy, 1997; Vorobjev *et al.*, 2001). In the cytoplasmic fragments, new MTs continuously grew from the pigment aggregate, indicating that in the absence of the centrosome, the pigment aggregate plays the role of the MT-organizing center. Therefore, in intact melanophores, nucleation of MTs on the emerging pigment granule aggregate could contribute to the increase in MT outgrowth from the cell center. However, it is not clear whether pigment granules can nucleate MTs at the low levels of free tubulin subunits found in intact cells (Rodionov *et al.*, 1999).

In this study, we developed an experimental strategy that allowed us to compare MT nucleation activity of the centrosome in two signaling states and determine the relative contribution of centrosomal and noncentrosomal mechanisms of MT nucleation to the increase in the number of MT tips available for the capture of pigment granules during pigment granule aggregation.

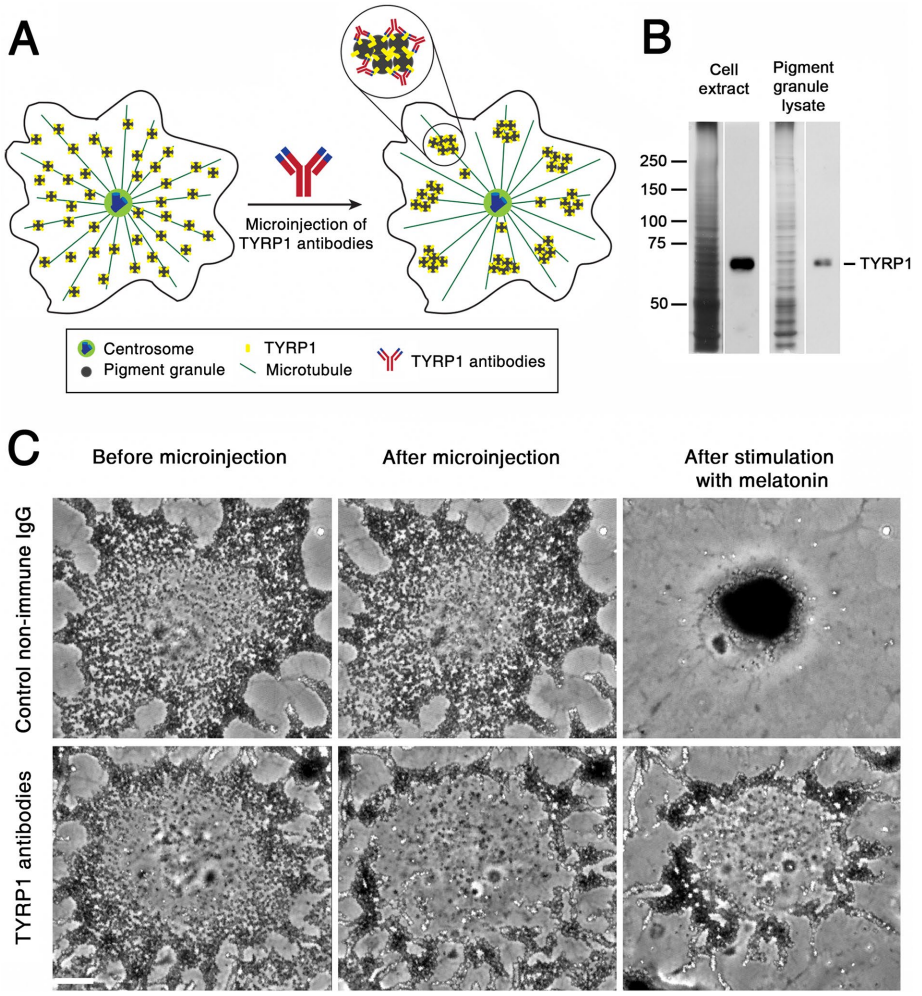

FIGURE 1: Microinjection of TYRP1 antibodies induces formation of pigment granule clusters with reduced ability to move to the cell center. (A) Design of a granule cross-linking experiment; antibodies against TYRP1 link neighboring pigment granules to each other, inducing formation of pigment granule clusters unable to efficiently move along MTs because of their large size. (B) Immunoblotting of cell extract (left) and lysate of pigment granules (right) with TYRP1 antibodies; left and right lanes of each pair correspond to silver-stained gels and immunoblots, respectively; in cell extract and lysate of pigment granules, antibodies recognize a single TYRP1 band with molecular mass of ~60 kDa. (C) Phase contrast images of melanophores microinjected with control nonimmune IgG (top) or TYRP1 antibodies (bottom) and treated to aggregate pigment granules; in each row, images show the distribution of pigment granules before (left) or 30 min after (middle) microinjection or 20 min after treatment of microinjected cells with melatonin to induce pigment aggregation (right); microinjection of control IgG does not significantly change the distribution of pigment granules and does not prevent their aggregation in the cell center, whereas microinjection of TYRP1 antibodies induces formation of peripheral granule clusters that fail to aggregate in the cell center after stimulation with melatonin; bar, 10 μm.

RESULTS AND DISCUSSION

To compare MT nucleation activity of the centrosome in two signaling states, we sought an experimental strategy that would prevent accumulation of pigment granules in the cell center. Pigment aggregation could be blocked by dynein inhibitors, but our previous work showed that inhibition of dynein activity affected the ability of the centrosome to establish a radial organization of MTs (Burakov *et al.*, 2008). Similarly, centripetal movement could be suppressed by binding of exogenous kinesin to pigment granules, but many pigment granules still reached the cell center, thus masking the centrosome region (Rezaul *et al.*, 2016). Therefore we chose an experimental strategy that did not rely on manipulation of MT motor activities but instead involved cross-linking pigment granules with each other using antibodies specific to a major granule protein (Figure 1A). We reasoned that antibody links would create granule clusters too large to be effectively transported by dynein motors to the cell center.

To cross-link pigment granules, we chose peptide antibodies against the cytoplasmic domain of tyrosinase-related protein 1 (TYRP1), an abundant pigment granule protein (Rezaul *et al.*, 2016) involved in the biosynthesis of melanin (del Marmol and Beermann, 1996). Immunoblotting of cell extracts and lysates of pigment granules showed that purified antibodies recognized a single band (Figure 1B) or two closely spaced bands (see Figure 4D later in this article) with molecular masses (~60 kDa) consistent with the molecular mass of TYRP1. For granule cross-linking, we injected TYRP1 antibodies into cells stimulated by the granule-dispersing melanocyte-stimulating hormone (MSH). Control experiments involved injection of melanophores with dispersed pigment granules with nonimmune immunoglobulin G (IgG) at the same needle concentration as TYRP1 antibodies. We found that,

as expected, microinjection of nonimmune IgG did not significantly alter the distribution of pigment granules (Figure 1C, top, and Supplemental Video S1). Furthermore, similar to noninjected cells (unpublished data) nonimmune IgG–injected melanophores aggregated pigment granules within 10–15 min after treatment with the granule-aggregating hormone melatonin (Supplemental Video S1). In striking contrast to nonimmune IgG, microinjection of TYRP1 antibodies induced rapid (5–10 min) formation of clumps of pigment granules at the cell periphery (Figure 1C, bottom, and Supplemental Video S2). Treatment of TYRP1 antibody–injected melanophores with melatonin (Supplemental Video S2, 20-min time point) caused centripetal movement of pigment granule clumps. However, the rate of their movement was slow compared with individual pigment granules, and therefore the cell center remained devoid of pigment granules for at least 30–40 min after the application of melatonin. Thus, in agreement with our expectations, in TYRP1 antibody–injected melanophores, the cell center was free of pigment granules for an extended period of time after stimulation of pigment aggregation, which allowed us to measure MT nucleation activity of the centrosome in this signaling state without the obstruction imposed by the pigment granule aggregate.

To measure MT nucleation activity of the centrosome and compare it between signaling states, we performed live fluorescence imaging of melanophores expressing enhanced green fluorescent protein (EGFP)–tagged EB1, a +Tip protein that specifically binds to the growing plus-ends of cytoplasmic MTs (Tirnauer *et al.*, 1999; Mimori-Kiyosue *et al.*, 2000). The number of EGFP-EB1–labeled segments of MTs (EB1 comets) emerging from the centrosome area provides a measure of the MT nucleation activity of the centrosome (Piehl *et al.*, 2004). To compare MT nucleation activity of the centrosome in two signaling states, we treated EGFP-EB1–expressing melanophores with MSH, microinjected the cells with TYRP1 antibodies, and acquired images of EGFP-EB1 comets before and after treatment with melatonin. For each cell, we quantified the number of comets surrounding the centrosome after treatment with MSH and melatonin. Remarkably, we found that the ratio of the average number of comets in the two states was 1.05 ± 0.05 (mean ± SEM; $n = 20$; Figure 2, bottom), an indication that pigment granule aggregation signals did not significantly enhance nucleation of MTs at the centrosome. To determine whether lack of stimulation of centrosomal MT nucleation could be explained by a nonspecific effect of microinjection, we injected EGFP-EB1–expressing cells treated with MSH with nonimmune rabbit IgG and counted the number of EGFP-EB1 comets in the same cells before and after stimulation with melatonin within the area surrounding the centrosome or placed in the center of the pigment aggregate (Figure 2, top). We found that the ratio of EGFP-EB1 comets in MSH- to melatonin-treated cells was 1.93 ± 0.19 (mean ± SEM; $n = 20$). This result was consistent with our previous data that showed that pigment aggregation signals induced approximately twofold increase in MT outgrowth from the cell center (Lomakin *et al.*, 2011) and ruled out a nonspecific effect of microinjection on MT nucleation. Taken together, the results of microinjection experiments indicate that the increase in number of MT plus ends growing from the cell center is not explained by stimulation of MT nucleation at the centrosome.

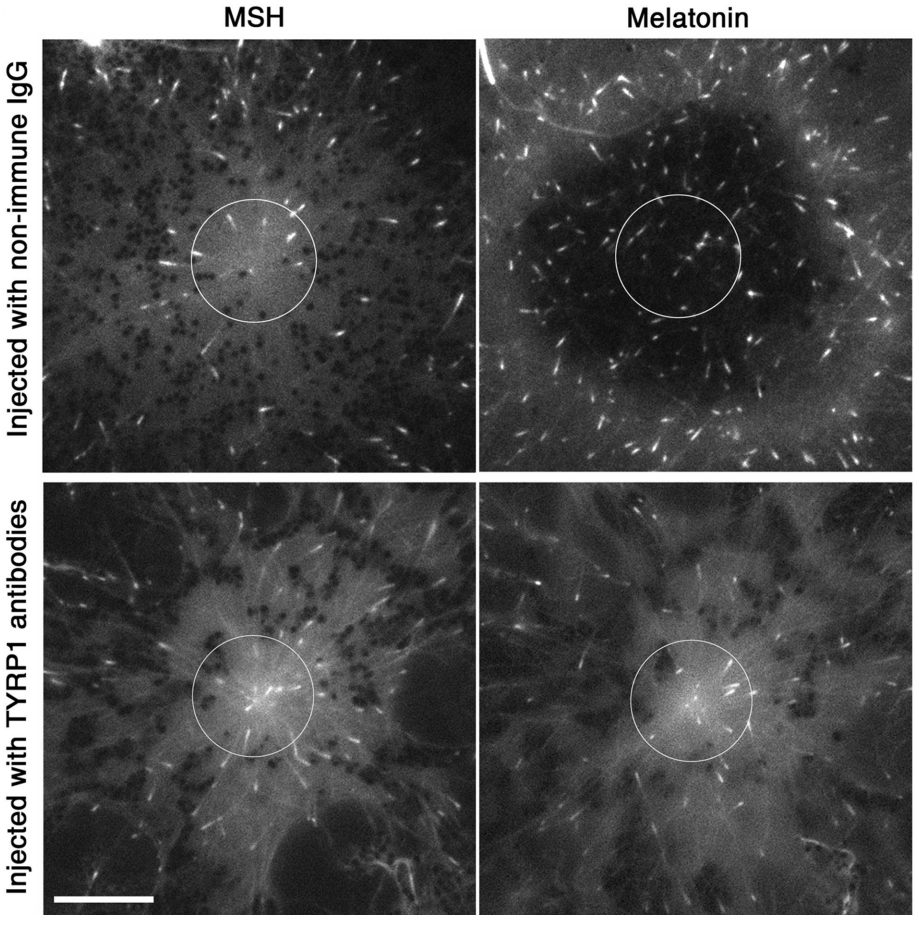

FIGURE 2: Pigment aggregation signals do not stimulate MT nucleation on the centrosome. Fluorescence images of melanophores expressing EGFP-EB1 injected with either control nonimmune IgG (top) or TYRP1 antibodies (bottom) treated with MSH (left) or melatonin (right); circles ($D = 12$ μm) outline the areas used for counting EGFP-EB1 comets; in the control cell, which aggregated pigment granules, melatonin treatment induced a significant increase in the number of EGFP-EB1 comets in the centrosome area, whereas in the TYRP1 antibody–injected cell, which did not accumulate pigment granules in the cell center, the number of comets surrounding the centrosome did not change significantly after stimulation with melatonin; bar, 10 μm.

The lack of stimulation of centrosomal MT nucleation by pigment aggregation signals suggested that an increase in the number of MTs growing to the cell periphery might be explained by the nucleation of MTs on pigment granules accumulating in the cell center. Inspection of time-lapse sequences of fluorescence images of melanophores expressing EGFP-EB1 and injected with TYRP1 antibodies revealed EGFP-EB1 comets that emerged from pigment granule clumps and moved toward the cell center (Figure 3A and Supplemental Video S3). This observation was consistent with nucleation of MTs on pigment granules cross-linked with TYRP1 antibodies. However, EGFP-EB1 comets moving to the cell center were sparse, and we did not observe a significant increase in their number in melatonin-treated cells (unpublished data), an

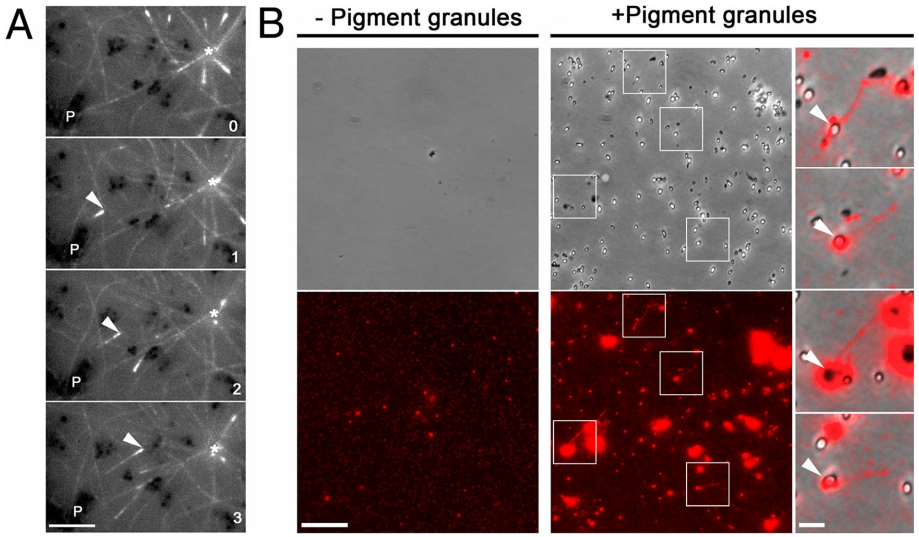

FIGURE 3: Pigment granules nucleate MTs in vivo and in vitro. (A) Sequential live fluorescence images of the centrosome area of an EGFP-EB1–expressing melanophore injected with TYRP1 antibodies and treated with melatonin; an asterisk indicates the position of the centrosome, P shows the location of a clump of pigment granules, and an arrowhead marks an EGFP-EB1 comet that emerges from the pigment granule clump and moves toward the centrosome; numbers indicate time in minutes. Birth of the MT tip labeled with EGFP-EB1 away from the centrosome and its growth toward the cell center suggest nucleation of the MT on a granule clump cross-linked with TYRP1 antibodies; bar, 2 μm. (B) Left and middle, phase contrast (top) and fluorescence (bottom) images of pellets of Cy3-labeled tubulin preparations incubated in the absence (left) or presence (right) of a suspension of purified pigment granules isolated from melanophores treated with melatonin to induce granule aggregation; right, overlays of boxed areas shown in the middle; tubulin pellets that were incubated in the presence of pigment granules contain short MTs that are often attached to pigment granules; bars, 10 μm (left and middle), 2 μm (right).

indication that binding of TYRP1 antibodies to pigment granules could inhibit MT nucleation. We therefore directly tested the MT-nucleation activity of pigment granules isolated from melatonin-treated melanophores. Isolated granules were incubated with preparations of chromatographically purified brain tubulin supplemented with a small amount of fluorescently labeled tubulin subunits and pelleted onto glass coverslips. Fluorescence microscopy of pigment granule pellets revealed several short MTs (Figure 3B, middle). An overlay of phase contrast images of pigment granules with fluorescence images of MTs showed that the ends of MTs were often attached to pigment granules (Figure 3B, right). MTs were never observed in the pellets of control samples obtained by incubation of tubulin preparations in the absence of pigment granules (Figure 3B). We conclude that pigment granules have MT-nucleation activity.

Pigment granules could continuously nucleate MTs at a constant rate, or their MT-nucleation activity could be stimulated by granule aggregation signals. To discriminate between these possibilities, we compared MT-nucleation activities of pigment granules isolated from melatonin- and MSH-treated cells by counting MTs in granule pellets obtained as described before (Figure 3B). To improve the accuracy of the measurements, we used preparations of tubulin partially purified from brain extracts by two cycles of reassembly and disassembly of MTs instead of chromatographically purified tubulin, and we visualized MTs in granule pellets by immunostaining with an α-tubulin antibody. Pellets of control tubulin samples incubated in the absence of pigment granules contained a few short MTs, consistent with the known capability of twice-cycled tubulin for a low level of spontaneous MT nucleation. The number of MTs in the pellets increased dramatically (~12-fold), however, when tubulin samples were incubated in the presence of granule preparations isolated from melatonin-treated cells (Figure 4, A and B). This result was consistent with the ability of pigment granules isolated from melatonin-treated melanophores to nucleate MTs (Figure 3B). Remarkably, in the presence of pigment granules isolated from cells treated with MSH, the number of MT increased to a much smaller extent (45.9 ± 1.4%, mean ± SEM of the average value determined for granules isolated from melatonin-treated cells; Figure 4, A and B), an indication of reduced MT nucleation activity. To confirm the results of MT-counting experiments, we used an alternative approach that measured MT polymer levels in granule pellets by quantitative immunoblotting with α-tubulin antibodies. The TYRP1 antibody signal from the same blots was also measured in order to normalize samples for the amounts of pigment granules. We detected a strong α-tubulin signal in the pellets of pigment granule preparations incubated with tubulin but not in the pellets of granule or tubulin samples incubated alone (Figure 4C). In full agreement with MT-counting data, α-tubulin levels were significantly higher (4.6 ± 0.6 times; mean ± SEM; $n = 5$) in the pellets of pigment granules isolated from cells treated with melatonin than with MSH (Figure 4C). Taken together, the results of these experiments indicated that that amount of MTs nucleated by pigment granules isolated from melatonin-treated cells was significantly larger than that of granules isolated from cells stimulated with MSH. We conclude that pigment granule aggregation signals increase MT-nucleation activity of pigment granules.

An increase in MT-nucleation activity of pigment granules could be explained by the activation of MT-nucleation templates permanently associated with pigment granules or by the recruitment of new MT-nucleation templates induced by granule aggregation signals. MT nucleation templates are generally provided by γ-tubulin ring complex (γ-TuRC; Zheng *et al.*, 1995), but nucleation on membrane organelles such as the Golgi complex requires other proteins (Wu *et al.*, 2016), including cytoplasmic linker associated protein (CLASP), which stabilizes minus ends of nascent MTs from disassembly (Efimov *et al.*, 2007). We therefore tested whether the major component of γ-TuRC, γ-tubulin, and CLASP were involved in nucleation of MTs on pigment granules and whether their levels were increased by granule-aggregating signals. To determine whether γ-tubulin and CLASP were bound to pigment granules, we attempted to localize them in melanophores by immunostaining with antibodies specific for each protein. However, we could not detect a significant fluorescence signal on pigment granules in cells containing or lacking (Rezaul *et al.*, 2016) melanin because of a high level of background cytoplasmic fluorescence. Therefore, to learn whether pigment granules bound γ-tubulin or CLASP, we used immunoblotting to probe preparations of isolated pigment granules with the relevant antibodies. We detected strong immunoblotting signals in preparations of pigment granules isolated from melatonin-treated cells, an indication that γ-tubulin and CLASP copurified with pigment granules (Figure 4D). To test whether each protein was involved in

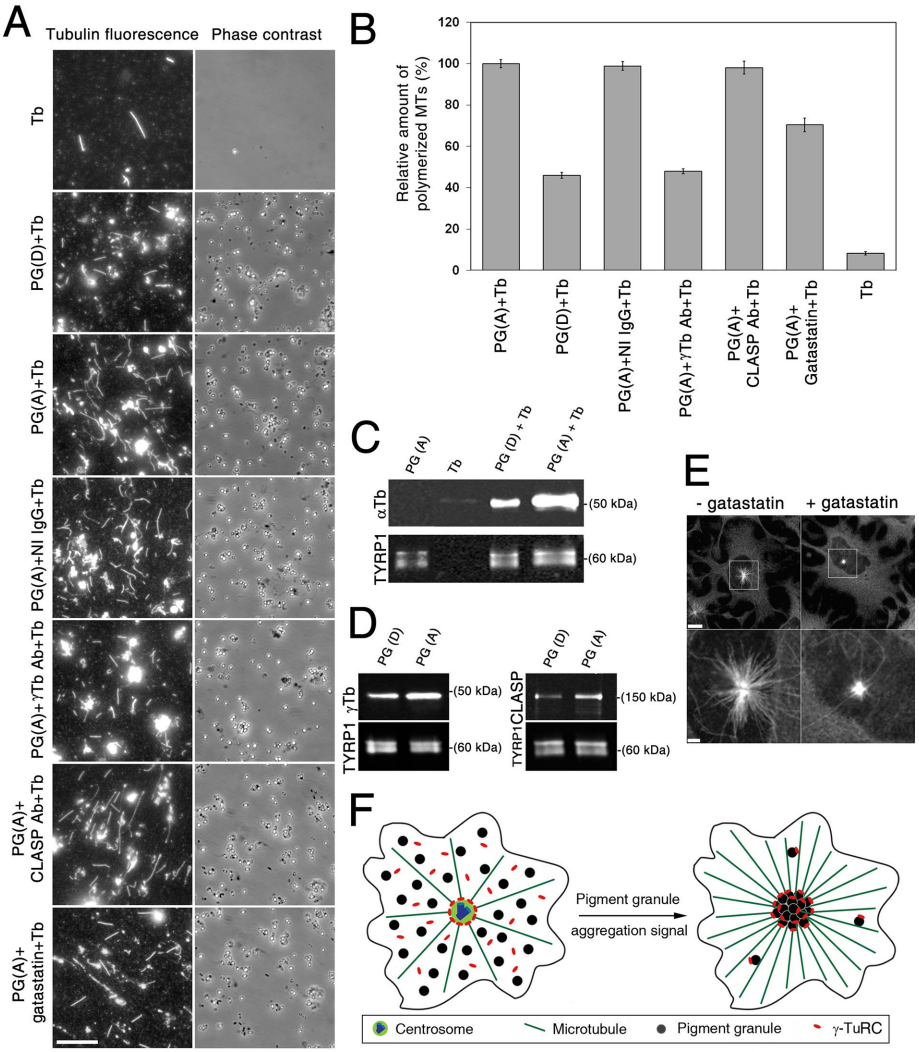

FIGURE 4: Pigment granule aggregation signals increase nucleation of MTs on pigment granules, and this increase correlates with the recruitment of γ-tubulin. (A) Fluorescence (left) and phase contrast (right) images of pellets of immunostained MTs assembled by polymerization of twice-cycled tubulin incubated alone or with different pigment granule preparations; shown are images from (Tb) alone, (PG(D)+Tb) pigment granules isolated from cells treated with MSH to induce granule dispersion, (PG(A)+Tb) pigment granules from cells treated with melatonin to trigger aggregation and preincubated with buffer only, (PG(A)+IgG+Tb) pretreated with nonimmune rabbit IgG, (PG(A)+ γ-Tb antibody+Tb) pretreated with γ-tubulin antibodies, (PG(A)+CLASP antibody+ Tb) pretreated with CLASP antibodies, or (PG(A)+gatastatin+Tb) pretreated with γ-tubulin inhibitor gatastatin. Pigment granules increased the amount of assembled MTs, and this effect was greater in the case of granules isolated from melatonin- compared with MSH-treated cells; preincubation of granules with γ-tubulin antibodies or gatastatin but not with nonimmune IgG or CLASP antibodies reduced the amount of assembled MTs; bar, 10 μm. (B) Quantification of the number of assembled MTs in samples shown in A; each bar represents the average value of 30 measurements in two independent experiments; the data are expressed as percentage of average number of MTs assembled in the presence of pigment granules isolated from melatonin-treated cells and incubated with relevant buffer, which is taken as 100%; error bars are mean ± SEM. (C) Comparison of MT nucleation activity of pigment granules isolated from melanophores treated with MSH or melatonin by immunoblotting of granule pellets with α-tubulin antibodies; blots with α-tubulin (top) or TYRP1 (bottom; loading control) antibodies of pellets from samples containing pigment granules isolated from melatonin-treated cells (PG(A)), purified tubulin (Tb), or mixtures of purified tubulin with pigment granules isolated from MSH- or melatonin-treated melanophores (PG(D)+Tb, and PG(A)+Tb, respectively); α-tubulin bands are absent from pellets of pigment granules or tubulin preparations (an indication that pigment granule preparations do not contain significant amounts of tubulin and that MTs do not assemble in the absence of pigment granules) but present in the pellets of mixtures of purified tubulin with pigment granules (an indication of MT nucleation on pigment granules); the amount of α-tubulin is significantly higher in the case of pigment granules isolated from melatonin-treated cells, suggesting stimulation of MT nucleation by the granule-aggregating signals. (D) Immunoblotting of preparations of purified pigment granules isolated from melanophores treated with MSH (left, PG(D)) or melatonin (right, PG(A)) with antibodies against γ-tubulin (left, top), CLASP (right, top) or TYRP1 (loading control; left and right, bottom); γ-tubulin and CLASP levels are increased in preparations of pigment granules isolated from melatonin-treated cells, which suggests that pigment-aggregation signals stimulate recruitment of γ-tubulin and CLASP to pigment granules. (E) Fluorescence images of melanin-free melanophores recovering from MT depolymerization in the absence (left) or presence (right) of gatastatin (30 μM); bottom, high-magnification images of boxed areas shown in the top; gatastatin partially inhibits MT outgrowth from the centrosome; bars, 10 μm (top), 2 μm (bottom). (F) Hypothesis on the stimulation of pigment aggregation by recruitment of γ-tubulin to pigment granules.

MT nucleation, we used the MT-counting routine to estimate the number of MTs assembled in preparations of pigment granules isolated from melatonin-treated cells and preincubated with γ-tubulin or CLASP antibodies. Control granule samples were preincubated with nonimmune IgG at the same concentration as antibodies specific for γ-tubulin or CLASP. We found that pretreatment of pigment granules with nonimmune IgG or CLASP antibodies did not significantly affect the average number of assembled MTs measured in control, nontreated samples. However, pretreatment of pigment granules with γ-tubulin antibodies reduced the average number of assembled MTs more than twofold (to 48.0 ± 1.3% of control levels), an indication that γ-tubulin was involved in MT nucleation. To confirm this result, we examined the effect on MT nucleation of the γ-tubulin inhibitor gatastatin (Chinen *et al.*, 2015). Control experiments indicated that, as expected, gatastatin partially inhibited MT outgrowth from the centrosome in melanophores recovering from treatment with cold and nocodazole (Figure 4E). Nucleation of MTs on pigment granules was also partially inhibited, as evidenced by a reduction of the number of MTs in granule pellets to 70.3 ± 3.2% of control levels (Figure 4, A and B). We concluded that nucleation of MTs on pigment granules involved γ-tubulin. To test whether pigment granule aggregation signals affected the levels of granule-bound

γ-tubulin, we used quantitative immunoblotting to compare the amounts of γ-tubulin in the pellets of pigment granules isolated from melatonin- and MSH-treated cells. We found that preparations of pigment granules isolated from melatonin-treated cells contained about twice (1.96 ± 0.12; mean ± SEM; $n = 8$) as much γ-tubulin as granule preparations isolated from MSH-treated melanophores (Figure 4D, left). We conclude that stimulation of MT nucleation by pigment granule aggregation signals is explained at least in part by recruitment of γ-tubulin to pigment granules.

In this study, we show that in *Xenopus* melanophores, pigment aggregation signals stimulate nucleation of MTs on pigment granules and that this stimulation is likely explained by recruitment of γ-tubulin to pigment granules. Our data are consistent with the results of several studies that demonstrated γ-tubulin–dependent nucleation of MTs on noncentrosomal nucleation sites (Bartolini and Gundersen, 2006; Petry and Vale, 2015). During mitosis, nucleation of MTs around chromatin, on kinetochores of chromosomes, and within the body of the mitotic spindle contributes to mitotic spindle morphogenesis (Petry and Vale, 2015). Similarly, in interphase cells, MTs are nucleated on the nuclear envelope in differentiating myoblasts and the cis-Golgi apparatus in locomoting cells (Bartolini and Gundersen, 2006; Petry and Vale, 2015; Sanders and Kaverina, 2015). Our work demonstrates for the first time that stimulation of MT nucleation on noncentrosomal MT-nucleation sites located on membrane organelles can be triggered by a distinct intracellular signal and occur on a time scale of a few minutes.

On the basis of the results of our experiments, we propose a model for the stimulation of centripetal transport of pigment granules along MTs during pigment aggregation in *Xenopus* melanophores (Figure 4F). We suggest that pigment aggregation signals stimulate binding of γ-TuRCs to pigment granules, increasing their MT nucleation activity. We hypothesize that each pigment granule binds small numbers of γ-TuRCs, and therefore the probability of MT nucleation on a single pigment granule is relatively low. However, accumulation of pigment granules in the cell center brings together multiple MT-nucleation templates, dramatically increasing the likelihood of MT nucleation. Gradual enlargement of the pigment aggregate leads to a progressive increase in the number of MT plus ends growing from the cell center, facilitating capture of pigment granules remaining in the peripheral cytoplasm. Therefore generation of new MT transport tracks by leading cargo organelles provides a positive feedback loop that enhances delivery of trailing organelles to the cell center.

MATERIALS AND METHODS

Cell culture

Xenopus melanophores (Ikeda *et al.*, 2010) were cultured in 70% L15 medium supplemented with 200 IU/ml penicillin, 200 µg/ml streptomycin, 2 mM glutamine, and 10% heat-inactivated fetal bovine serum (Life Technologies, Grand Island, NY) at 27°C. Before aggregation or dispersion of pigment granules, melanophores were incubated for 1–3 h at 27°C in serum-free medium (70% L15 medium supplemented with antibiotics and glutamine). To deplete cells of melanin, tissue culture medium was supplemented with 1 mM phenylthiourea (Rezaul *et al.*, 2016). Aggregation and dispersion of pigment granules were induced with 10^{-8} M melatonin and 10^{-8} M MSH, respectively.

Transfection

For expression of EGFP-EB1 (Stepanova *et al.*, 2003), melanophores were transfected using GeneCellin transfection reagent (Bulldog Bio, Portsmouth, NH) according to instructions provided by the manufacturer.

Microinjection of melanophores with TYRP1 antibodies or control nonimmune IgG

TYRP1 antibodies were produced by immunizing rabbits with a synthetic peptide that corresponded to the C-terminal amino acid sequence of the *Xenopus laevis* TYRP1 (Rezaul *et al.*, 2016). Antibodies were purified by affinity chromatography on an agarose column with covalently linked antigen and dialyzed against microinjection buffer (114 mM KCl, 20 mM NaCl, 3 mM $MgCl_2$, 3 mM NaH_2PO_4, pH 7.0). Lyophilized control nonimmune rabbit IgG (Sigma-Aldrich, St. Louis, MO) was dissolved in the same buffer. Pressure microinjection was performed as described previously (Semenova and Rodionov, 2007) using a Nikon TE300 inverted microscope equipped with mechanical micromanipulator (Leica Microsystems, Buffalo Grove, IL) and picoliter microinjector (Harvard Apparatus, Holliston, MA). Needle concentrations of TYRP1 antibodies and nonimmune rabbit IgG were ~15 mg/ml.

Isolation of pigment granules

Pigment granules were isolated as described previously (Kashina *et al.*, 2004). Briefly, cells were washed with 0.7× phosphate-buffered saline supplemented with 1 mM dithiothreitol and protease and phosphatase inhibitor cocktails (Sigma-Aldrich). Cells were harvested using a cell scraper into 0.5 ml of IMB50 buffer (50 mM imidazole, pH 7.4, 5 mM magnesium acetate, 1 mM ethylene glycol tetraacetic acid [EGTA], 175 mM sucrose, 0.5 mM EDTA) supplemented with protease and phosphatase inhibitor cocktails and lysed by passing seven times through a $27^{1/4}$-gauge hypodermic needle. Cell debris was removed by centrifugation at 210 × *g* for 10 min, and pigment granules were purified by centrifugation at 1750 × *g* for 10 min through a 5% sucrose solution prepared in IMB50 buffer supplemented with protease and phosphatase inhibitor cocktails.

MT nucleation on pigment granules in vitro

For detection of MT nucleation activity of pigment granules by MT fluorescence, a suspension of pigment granules isolated from melatonin-treated melanophores was incubated in the presence of a ~1:10 mixture of Cy3-labeled (Semenova and Rodionov, 2007) and unlabeled (Cytoskeleton Denver, CO) chromatographically purified porcine brain tubulin preparations (final total tubulin concentration 0.5 mg/ml). Incubation was performed in BRB80 buffer (80 mM 1,4-piperazinediethanesulfonic acid, 1 mM $MgCl_2$, 1 mM EGTA, pH 6.8) containing 1 mM GTP for 15 min at 20°C and 30 min at 29°C (Ori-McKenney *et al.*, 2012). After incubation, suspension was diluted 10-fold with BRB80 buffer containing 1% glutaraldehyde and incubated 3 min at room temperature for the fixation of assembled MTs. Pigment granules were then sedimented onto polylysine-coated coverslips by centrifugation through 5% sucrose in BRB80 buffer at 1750 × *g* for 15 min at 4°C, and granule pellets were examined using a fluorescence microscope.

For quantification of MT-nucleation activity of pigment granules by counting fluorescent MTs, granule suspension was incubated for 5 min at 37°C (Vinh *et al.*, 2002) in the presence of 0.2 mg/ml tubulin isolated from bovine brain by two cycles of reassembly and disassembly of MTs. After glutaraldehyde fixation and pelleting onto polylysine-coated coverslips, MTs were immunostained with α-tubulin antibodies (DM1A; Cedarlane, Burlington, Canada) and Alexa 488–conjugated goat anti-mouse antibodies (Thermo Fisher Scientific, Waltham, MA). Images of MTs were acquired using a fluorescence microscope and used for MT counting.

To examine the roles of γ-tubulin or CLASP in MT nucleation, a concentrated suspension of pigment granules was incubated in the presence of the γ-tubulin inhibitor gatastatin (30 μM), antibodies against γ-tubulin or CLASP (1.5 mg/ml each), or control rabbit nonimmune IgG (1.5 mg/ml; Sigma-Aldrich) in BRB80 buffer for 30 min at room temperature. The granule suspension was then diluted 16-fold with BRB80 buffer and incubated with twice-cycled tubulin for MT assembly as described. Polyclonal antibodies against γ-tubulin were produced by immunization of rabbits with the synthetic peptide EEFATEGTDRKDVFFY. For generation of function-blocking (Hannak and Heald, 2006) antibodies against CLASP, a fragment of *Xenopus* CLASP that corresponded to 282 C-terminal amino acid residues fused to glutathione *S*-transferase was expressed in *Escherichia coli*, purified by chromatography on glutathione Sepharose 4B (GE Healthcare Bio-sciences, Pittsburgh, PA), and used for immunization of rabbits (Hannak and Heald, 2006). Antibodies were purified from rabbit sera by affinity chromatography on agarose columns with covalently attached antigens. Immunoblotting indicated that in extracts of melanophores, purified antibodies recognized major bands with electrophoretic mobilities consistent with molecular masses of relevant proteins.

For quantification of MT-nucleation activity of pigment granules by measurement of tubulin levels in granule pellets, a suspension of purified pigment granules was incubated with chromatographically purified porcine brain tubulin (Cytoskeleton) and centrifuged through a solution of 33% glycerol in BRB80 buffer at 1750 × *g* for 10 min at 37°C. Pellets were extracted with SDS–PAGE sample buffer and granule extracts used for measurement of tubulin levels by quantitative immunoblotting with α-tubulin antibody.

Regrowth of MTs from the centrosome in vivo in the presence of gatastatin

The effect of gatastatin on regrowth of MTs from the centrosome was examined as described previously (Chinen *et al.*, 2015). Melanophores devoid of melanin and with MTs disrupted by sequential treatment with nocodazole and cold were incubated in the tissue culture medium containing 1% dimethyl sulfoxide (DMSO) or 30 μM gatastatin for 10 min on ice. Cells were then placed in tissue culture medium prewarmed to 37°C containing either 1% DMSO or 30 μM gatastatin, incubated for 5 min at 37°C, fixed with cold methanol, and immunostained by incubating with α-tubulin antibodies (DM1A; Cedarlane) and Alexa 488–conjugated goat anti-mouse antibodies (Thermo Fisher Scientific).

Image acquisition and analysis

Time-sequences of phase contrast images of melanophores were acquired using a Nikon TE300 inverted microscope with a Watec 902B charge-coupled device (CCD) video camera (Watec Cameras, Japan) driven by MetaMorph image acquisition and analysis software (Universal Imaging, Downington, PA). Live fluorescence microscopy of cells expressing EGFP-EB1 or in vitro–assembled MTs was performed using a Nikon Eclipse Ti inverted microscope equipped with a 100×/numerical aperture 1.4 Plan Apochromat objective lens. Fluorescence images were acquired with an iXon electron-multiplying CCD camera (Andor Technology, Windsor, CT) driven by MetaMorph software.

To compare MT nucleation activity of the centrosome in two signaling states, melanophores expressing EGFP-EB1 were treated with MSH to disperse pigment granules, injected with TYRP1 antibodies, and incubated for 30 min to allow for cross-linking of pigment granules. Time sequences of 60 fluorescence images of EGFP-EB1 comets in the centrosome area were acquired with a 3-s time interval. Cells were then thoroughly washed with serum-free tissue culture medium to remove excess MSH and treated with melatonin for 15 min, and a second time sequence was acquired in the same area. EGFP-EB1 comets were counted within a circular region (D = 12 μm) surrounding the centrosome or placed in the center of the pigment aggregate in each of the five frames of a time-lapse sequence separated by 1-min time intervals. The data were averaged across each time sequence and used to calculate the ratio of average comet numbers in the same cells treated with melatonin and MSH.

To measure MT-nucleation activity of isolated pigment granules in vitro, images of fluorescent MTs pelleted onto carbon-coated coverslips were captured using an 100× objective lens and an additional 1.5× lens inserted in the optical path of the microscope, and MTs in each sample were counted in 15 random fields of view. For each experimental condition, MT counts were obtained in two independent experiments. The data were averaged and expressed as a percentage of average MT counts in control samples that were obtained by incubation of tubulin in the presence of pigment granules that were not pretreated with gatastatin or γ-tubulin or CLASP antibodies.

Quantitative immunoblotting

For quantitative immunoblotting, protein bands separated using SDS–PAGE were transferred onto nitrocellulose membrane and stained with primary antibodies and IRDye800-conjugatged, affinity-purified anti-mouse or anti-rabbit secondary antibodies (Rockland Immunochemicals, Pottstown, PA). Primary antibodies were commercially available monoclonal antibodies against γ-tubulin (GTU-88; Sigma-Aldrich) or α-tubulin (DM1A; Cedarlane Laboratories) or polyclonal affinity-purified antibodies against TYRP1 (Rezaul *et al.*, 2016) or *Xenopus* CLASP. The intensity of the infrared signal was quantified with the Odyssey Infrared Imaging System (Li-Cor Biosciences, Lincoln, NE). All measured integrated intensities of protein bands fell into the linear range. To compare levels of α-tubulin, γ-tubulin, or CLASP between preparations of pigment granules isolated from cells treated to aggregate or disperse pigment granules, pigment granule lysates were normalized to the amounts of TYRP1 that were quantified in an independent immunoblotting experiment.

ACKNOWLEDGMENTS

We thank Rebecca Heald for *Xenopus* CLASP cDNA. This work was supported by National Institutes of Health Grant GM62290 to V.R.

REFERENCES

Akhmanova A, Hammer JA 3rd (2010). Linking molecular motors to membrane cargo. Curr Opin Cell Biol 22, 479–487.

Barlan K, Rossow MJ, Gelfand VI (2013). The journey of the organelle: teamwork and regulation in intracellular transport. Curr Opin Cell Biol 25, 483–488.

Bartolini F, Gundersen GG (2006). Generation of noncentrosomal microtubule arrays. J Cell Sci 119, 4155–4163.

Burakov A, Kovalenko O, Semenova I, Zhapparova O, Nadezhdina E, Rodionov V (2008). Cytoplasmic dynein is involved in the retention of microtubules at the centrosome in interphase cells. Traffic 9, 472–480.

Caviston JP, Holzbaur EL (2006). Microtubule motors at the intersection of trafficking and transport. Trends Cell Biol 16, 530–537.

Chinen T, Liu P, Shioda S, Pagel J, Cerikan B, Lin TC, Gruss O, Hayashi Y, Takeno H, Shima T, *et al.* (2015). The gamma-tubulin-specific inhibitor gatastatin reveals temporal requirements of microtubule nucleation during the cell cycle. Nat Commun 6, 8722.

del Marmol V, Beermann F (1996). Tyrosinase and related proteins in mammalian pigmentation. FEBS Lett 381, 165–168.

Efimov A, Kharitonov A, Efimova N, Loncarek J, Miller PM, Andreyeva N, Gleeson P, Galjart N, Maia AR, McLeod IX, *et al.* (2007). Asymmetric CLASP-dependent nucleation of noncentrosomal microtubules at the trans-Golgi network. Dev Cell 12, 917–930.
Flory MR, Moser MJ, Monnat RJ Jr, Davis TN (2000). Identification of a human centrosomal calmodulin-binding protein that shares homology with pericentrin. Proc Natl Acad Sci USA 97, 5919–5923.
Fu MM, Holzbaur EL (2014). Integrated regulation of motor-driven organelle transport by scaffolding proteins. Trends Cell Biol 24, 564–574.
Hannak E, Heald R (2006). Xorbit/CLASP links dynamic microtubules to chromosomes in the Xenopus meiotic spindle. J Cell Biol 172, 19–25.
Ikeda K, Semenova I, Zhapparova O, Rodionov V (2010). Melanophores for microtubule dynamics and motility assays. Methods Cell Biol 97, 401–414.
Kapitein LC, Hoogenraad CC (2011). Which way to go? Cytoskeletal organization and polarized transport in neurons. Mol Cell Neurosci 46, 9–20.
Kashina A, Rodionov V (2005). Intracellular organelle transport: few motors, many signals. Trends Cell Biol 15, 396–398.
Kashina AS, Semenova IV, Ivanov PA, Potekhina ES, Zaliapin I, Rodionov VI (2004). Protein kinase A, which regulates intracellular transport, forms complexes with molecular motors on organelles. Curr Biol 14, 1877–1881.
Li Q, Hansen D, Killilea A, Joshi HC, Palazzo RE, Balczon R (2001). Kendrin/pericentrin-B, a centrosome protein with homology to pericentrin that complexes with PCM-1. J Cell Sci 114, 797–809.
Lomakin AJ, Kraikivski P, Semenova I, Ikeda K, Zaliapin I, Tirnauer JS, Akhmanova A, Rodionov V (2011). Stimulation of the CLIP-170–dependent capture of membrane organelles by microtubules through fine tuning of microtubule assembly dynamics. Mol Biol Cell 22, 4029–4037.
Lomakin AJ, Semenova I, Zaliapin I, Kraikivski P, Nadezhdina E, Slepchenko BM, Akhmanova A, Rodionov V (2009). CLIP-170-dependent capture of membrane organelles by microtubules initiates minus-end directed transport. Dev Cell 17, 323–333.
Mimori-Kiyosue Y, Shiina N, Tsukita S (2000). The dynamic behavior of the APC-binding protein EB1 on the distal ends of microtubules. Curr Biol 10, 865–868.
Ori-McKenney KM, Jan LY, Jan YN (2012). Golgi outposts shape dendrite morphology by functioning as sites of acentrosomal microtubule nucleation in neurons. Neuron 76, 921–930.
Petry S, Vale RD (2015). Microtubule nucleation at the centrosome and beyond. Nat Cell Biol 17, 1089–1093.
Piehl M, Tulu US, Wadsworth P, Cassimeris L (2004). Centrosome maturation: measurement of microtubule nucleation throughout the cell cycle by using GFP-tagged EB1. Proc Natl Acad Sci USA 101, 1584–1588.
Rezaul K, Gupta D, Semenova I, Ikeda K, Kraikivski P, Yu J, Cowan A, Zaliapin I, Rodionov V (2016). Engineered tug-of-war between kinesin and dynein controls direction of microtubule based transport in vivo. Traffic 17, 475–486.
Rodionov V, Nadezhdina E, Borisy G (1999). Centrosomal control of microtubule dynamics. Proc Natl Acad Sci USA 96, 115–120.
Rodionov VI, Borisy GG (1997). Self-centring activity of cytoplasm. Nature 386, 170–173.
Sanders AA, Kaverina I (2015). Nucleation and dynamics of Golgi-derived microtubules. Front Neurosci 9, 431.
Semenova I, Rodionov V (2007). Fluorescence microscopy of microtubules in cultured cells. Methods Mol Med 137, 93–102.
Stepanova T, Slemmer J, Hoogenraad CC, Lansbergen G, Dortland B, De Zeeuw CI, Grosveld F, van Cappellen G, Akhmanova A, Galjart N (2003). Visualization of microtubule growth in cultured neurons via the use of EB3-GFP (end-binding protein 3-green fluorescent protein). J Neurosci 23, 2655–2664.
Takahashi M, Mukai H, Oishi K, Isagawa T, Ono Y (2000). Association of immature hypophosphorylated protein kinase cepsilon with an anchoring protein CG-NAP. J Biol Chem 275, 34592–34596.
Terrin A, Monterisi S, Stangherlin A, Zoccarato A, Koschinski A, Surdo NC, Mongillo M, Sawa A, Jordanides NE, Mountford JC, Zaccolo M (2012). PKA and PDE4D3 anchoring to AKAP9 provides distinct regulation of cAMP signals at the centrosome. J Cell Biol 198, 607–621.
Tirnauer JS, O'Toole E, Berrueta L, Bierer BE, Pellman D (1999). Yeast Bim1p promotes the G1-specific dynamics of microtubules. J Cell Biol 145, 993–1007.
Vale RD (2003). The molecular motor toolbox for intracellular transport. Cell 112, 467–480.
Verhey KJ, Hammond JW (2009). Traffic control: regulation of kinesin motors. Nat Rev Mol Cell Biol 10, 765–777.
Vinh DB, Kern JW, Hancock WO, Howard J, Davis TN (2002). Reconstitution and characterization of budding yeast gamma-tubulin complex. Mol Biol Cell 13, 1144–1157.
Vorobjev I, Malikov V, Rodionov V (2001). Self-organization of a radial microtubule array by dynein-dependent nucleation of microtubules. Proc Natl Acad Sci USA 98, 10160–10165.
Walczak CE, Cai S, Khodjakov A (2010). Mechanisms of chromosome behaviour during mitosis. Nat Rev Mol Cell Biol 11, 91–102.
Witczak O, Skalhegg BS, Keryer G, Bornens M, Tasken K, Jahnsen T, Orstavik S (1999). Cloning and characterization of a cDNA encoding an A-kinase anchoring protein located in the centrosome, AKAP450. EMBO J 18, 1858–1868.
Wu J, de Heus C, Liu Q, Bouchet BP, Noordstra I, Jiang K, Hua S, Martin M, Yang C, Grigoriev I, *et al.* (2016). Molecular pathway of microtubule organization at the Golgi apparatus. Dev Cell 39, 44–60.
Zheng Y, Wong ML, Alberts B, Mitchison T (1995). Nucleation of microtubule assembly by a gamma-tubulin-containing ring complex. Nature 378, 578–583.